Supplementary Information for

S1. Various concave-convex graphene-SiO_2 laminates.

Figure S1 shows scanning electron microscopy (SEM) images of a variety of concave-convex graphene-SiO_2 laminates with different geometries: a square convex pattern with a size of 10 μm × 10 μm (Figure S1a), a circular convex pattern with a diameter of 10 μm (Figure S1b), a "squircle" or oval convex pattern with a size of 8 μm × 3 μm (Figure S1c), a circular convex pattern with a diameter of 5 μm (Figure S1d), elongated rod convex patterns with a size of 3 μm × 45 μm and with inter-pattern distances of 3 (Figure S1e) and 6 μm (Figure S1f), convex (Figure S1g) and concave (Figure S1h) zig-zag patterns with a size of 3 μm × 12 μm, and a circular concave pattern with a diameter of 5 μm (Figure S1i).

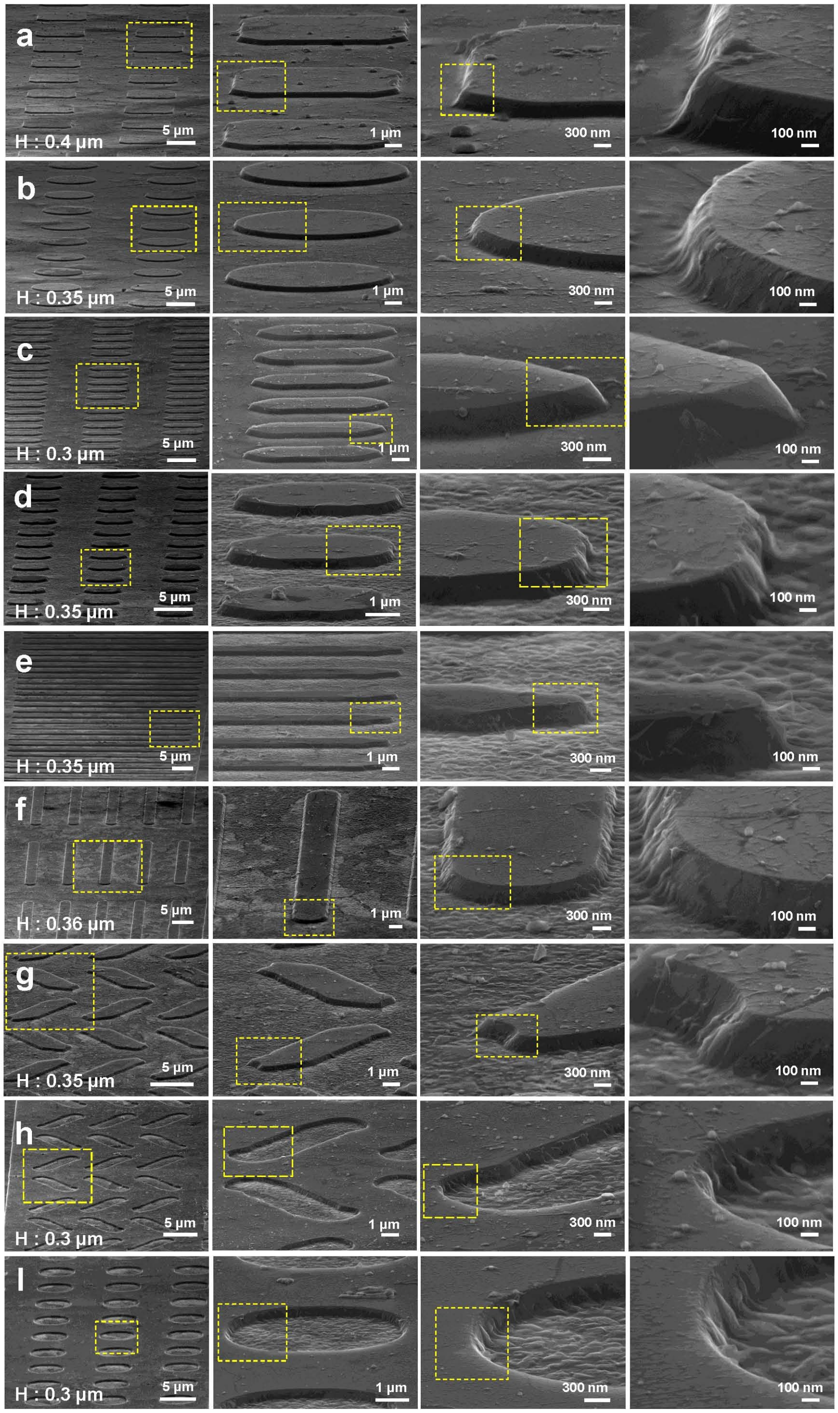

Figure S1. (a-g) SEM images of convex graphene-SiO_2 laminates. (h-i) SEM images of concave graphene-SiO_2 laminates. The yellow dashed rectangular regions are shown in the magnified images, where H is the height of the architecture.

S2. Scanning electron microscopy images before and after the 3D lamination

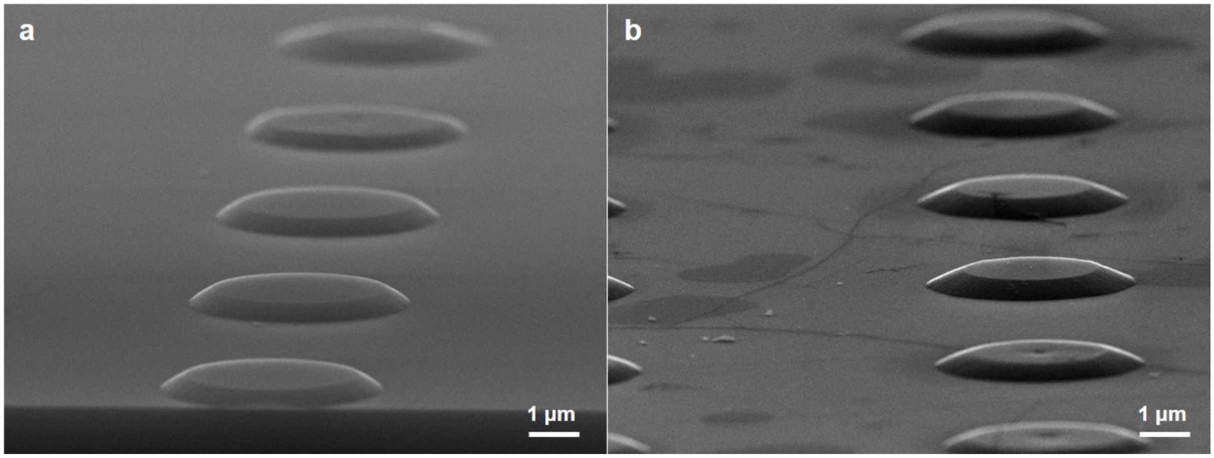

Figure S2. (a) A SEM image of a convex SiO_2 structure before the 3D lamination. (b) A SEM image of a convex graphene-SiO_2 laminate after the 3D lamination,

S3. Influence of the size and gradient of the convex SiO_2 architecture on graphene lamination

To investigate the effect of the size of the SiO_2 architecture on the graphene laminates, the diameters of circular convex SiO_2 patterns with the same height of 300 nm were varied at 4.4 μm (Figure S3a) and 9.4 μm (Figure S3b). To study the influence of the gradient of the SiO_2 architecture on the lamination, the gradients of circular convex SiO_2 patterns with the same thickness of 300 nm were changed (Figures S3c,d).

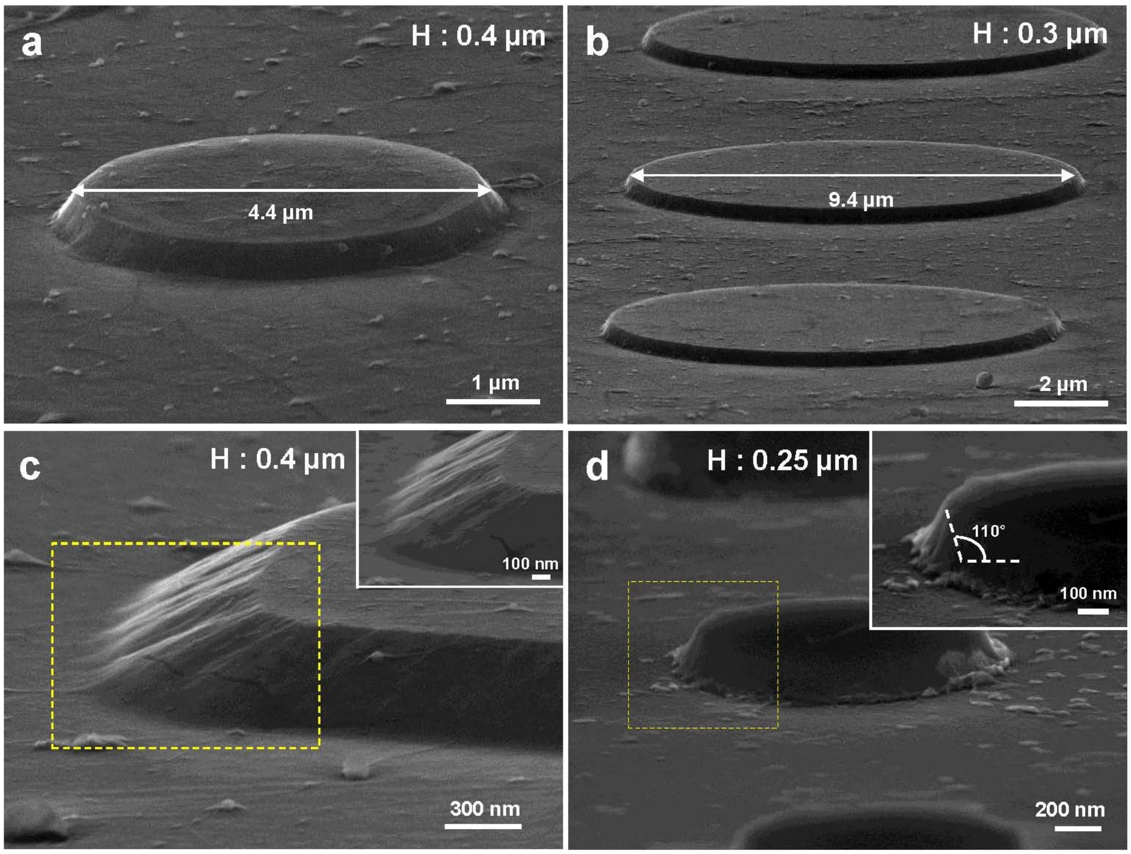

Figure S3. (a-d) SEM images of convex graphene-SiO_2 laminates with different diameters and gradients. In (c-d), the yellow dashed rectangular regions were magnified and inserted as insets, where H is the height of the architecture.

S4. Influence of the gradient of the convex SiO_2 architecture on graphene lamination

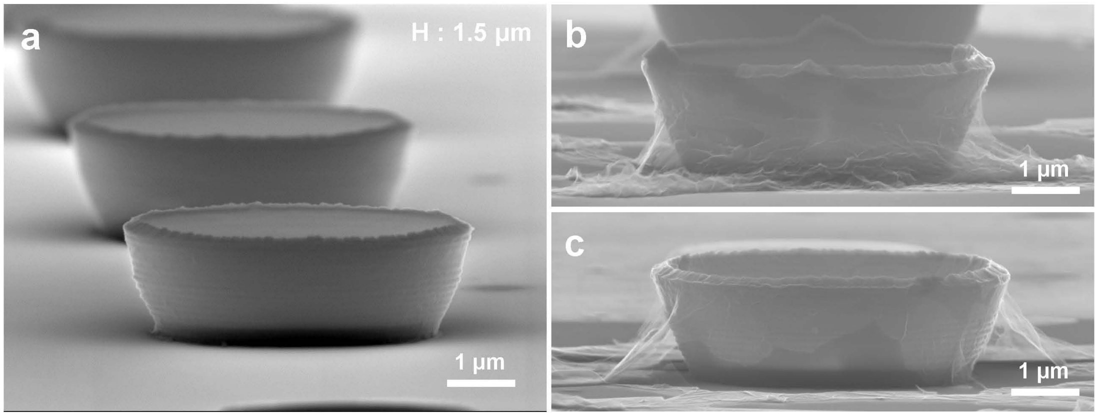

Figure S4. SEM images before (a) and after (b) the lamination of graphene for the architecture with an inclination angle above 90°, where H is the height of the architecture.

S5. The thicknesses of PMMA films coated

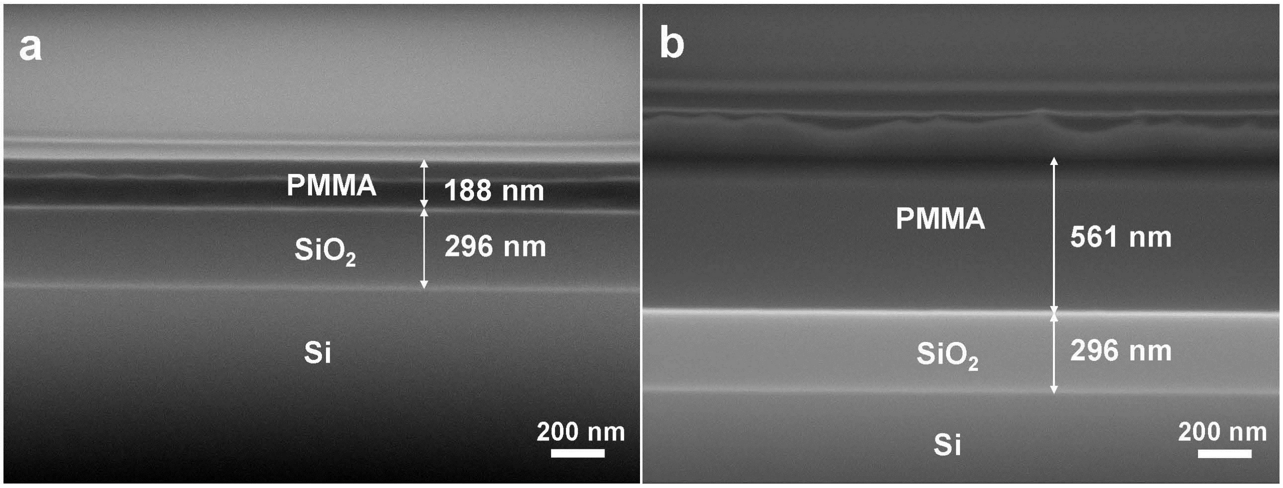

Figure S5. (a-b) Cross-sectional SEM images of PMMA-coated SiO_2/Si wafers. The thickness of the PMMA film in (a) is equal to that of a PMMA film used for the transfer of PMMA-coated graphene onto a 3D architecture. The thickness of the PMMA film in (b) is equal to that of a total PMMA film used for the lamination of a 3D architecture, where an additional liquid PMMA film was spin-coated on the PMMA film of (a).

S6. Spatial distributions of chemical configurations on graphene on the 3D laminate

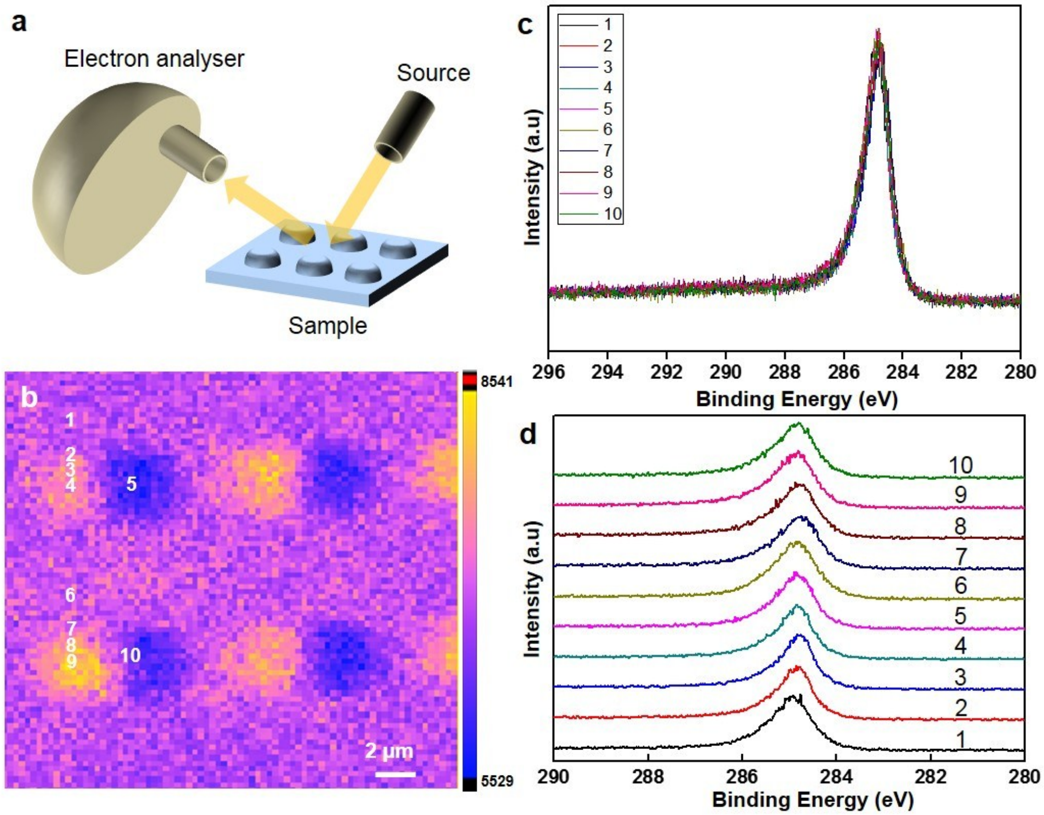

Figure S6. (a) The schematic drawing of scanning photoemission microscopy (SPEM). (b) The SPEM image of photoelectron intensity with a binding energy window between 280 and 292 eV, where a photon beam of 630 eV was focused at the top of the 3D laminate during the scanning. (c-d) Spatially-resolved C 1*s* spectra, where the positions of the spectra are indicated by the number in (b). The spatially-resolved C 1*s* are overlapped in (c) and spread out in (d).

S7. Calculations of average strain (%)

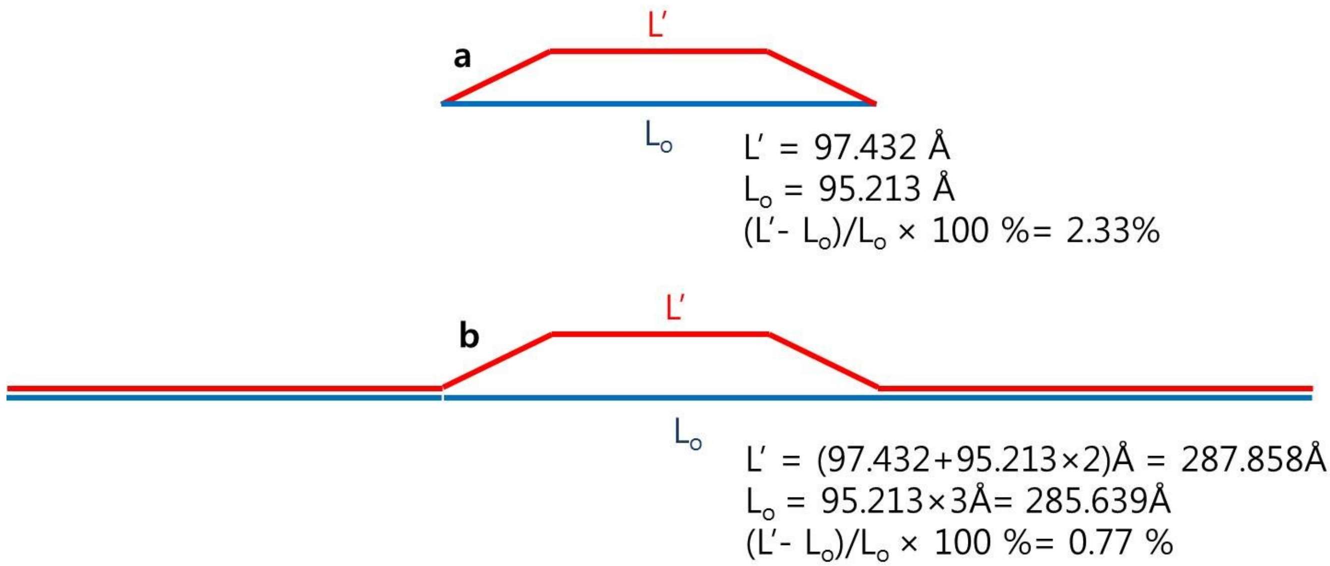

Figure S7. (a-b) The average strain (%) of the 3D graphene used in the MD simulations (Figure 4), where L_o and L' are lengths before and after the lamination, respectively, where the average strain is $(L' - L_o)/L_o \times 100$ %. In (a), the average strain is calculated when graphene at the bottom is fixed. In (b), the average strain is calculated when graphene at the bottom can be relaxed, for example.